Journal of Engineering for Gas Turbines and Power, Volume 144, Issue 7, July 2022, Paper number GTP-21-1595
DOI:10.1115/1.4054405

Assessment of performance boundaries and operability of low specific thrust GUHBPR engines for EIS2025

Da Mo[1]
AECC Shenyang Engine Research Institute, Shenyang, 110015, China

Ioannis Roumeliotis[2]
Centre for Propulsion Engineering, School of Aerospace, Transport and Manufacturing, Cranfield University, Bedfordshire, MK43 0AL, United Kingdom

and
Christos Mourouzidis[3], Sajal Kissoon[4]
Centre for Propulsion Engineering, School of Aerospace, Transport and Manufacturing, Cranfield University, Bedfordshire, MK43 0AL, United Kingdom

Yixiong Liu[5]
AECC Shenyang Engine Research Institute, Shenyang, 110015, China

This paper aims to develop a robust design process by approaching the performance boundaries and evaluating the operability of the pursued geared turbofan engine with low specific thrust for EIS 2025. A two-spool direct-drive turbofan (DDTF) engine of EIS 2000 was improved according to aircraft specifications and technology boundaries in 2025. A series of optimized engines with consecutive fan diameters were established to seek the ideal engine by balancing SFC, weight and mission fuel burn. The fan diameter was proved to be a decisive factor for lowering SFC and energy usage. The cycle design optimization process achieved a thermal efficiency of approximately 52%, and a propulsive efficiency of 79.5%, which is 8.19% increase in propulsive efficiency by enlarging fan diameter from 1.6m to 1.9m. Meanwhile, the 1.9m-fan diameter engine achieved a reduction in SFC and fuel burn of 7.47% and 6.58% respectively which offers an overall reduction of 30.82% in block fuel burnt and CO2 emission compared to the DDTF engine. A feasibility check verified the

[1] Senior Engineer, AECC Shenyang Engine Research Institute.Corresponding author, dada1204@126.com.
[2] Senior Lecturer, Cranfield University.
[3] Lecturer, Cranfield University.
[4] Research Fellow, Cranfield University.
[5] Senior Engineer, AECC Shenyang Engine Research Institute.

viability of the designed optimum engine in terms of fan tip speed, stage loading and AN^2. Dynamic simulation offered a deep understanding of transient behaviour and fundamental mechanism of the geared turbofan engine. An important aspect of this paper is the use of advanced CMC materials, which led to an improvement of 4.92% in block fuel burn and 2.93% in engine weight.

Nomenclature

Roman symbols

A_{fan}	Fan inlet area
AN^2	Turbine Area Times Rotational Speed Squared
B_{fuel}	Block Fuel
C	Constant
D_{fan}	Fan Diameter
E_{weight}	Engine Weight
Fs	Specific Thrust
FPR_{op}	Optimum Fan Pressure Ratio
h_{HPC}	HPC Last Stage Blade Height
n_{stage}	Stage Count
P3	HPC Exit Pressure
T3	HPC Exit Temperature
T4	Combustion Outlet Temperature
T41	Turbine Inlet Temperature
Tbl	Turbine Blade Mean Metal Temperature
Tg	Hot Gas Temperature
Utip	Fan Tip Speed
W_2	Intake Air Mass Flow
W^+	Temperature Difference Ratio

Greek symbols

ε_F	Film Cooling Effectiveness
ε_o	Overall Cooling Effectiveness
η_{cool}	Cooling Efficiency
η_{poly}	Polytropic Efficiency
η_{prop}	Propulsive Efficiency
η_{th}	Thermal Efficiency

ρ	Density
φ	Cooling Air Fraction
ψ_{fan}	Fan Average Stage Loading
ψ_{LPT}	LPT Average Stage Loading

Acronyms

ACARE	Advisory Council for Aviation Research in Europe
BPR	Bypass Ratio
BOV	Blow-Off Valve
CMC	Ceramic Matrix Composites
CR	Cruise
DDTF	Direct Drive Turbofan
DP	Design Point
EIS	Enter Into Service
FLOPS	Flight Optimization System
FPR	Fan Pressure Ratio
GTF	Geared Turbofan
GR	Gear Ratio
HPC	High-Pressure Compressor
HPT	High-Pressure Turbine
IP	Intermediate Pressure
IPC	Intermediate Pressure Compressor
ISA	International Standard Atmosphere
LP	Low Pressure
LPT	Low-Pressure Turbine
MEW	Maximum Empty Weight
MRW	Maximum Ramp Weight
MTOW	Maximum Take-Off Weight
NGV	Nozzle Guide Vane
OPR	Overall Pressure Ratio
OEW	Operating Empty Weight
PGB	Power Gearbox
PR	Pressure Ratio
SFC	Specific Fuel Consumption
SLS	Static Level Sea
TO	Take-Off

ToC	Top of Climb
VAN	Variable Area Nozzle
VIGV	Variable Inlet Guide Vane
VPF	Variable Pitch Fan

I. Introduction

Nowadays, the increase in airline costs and fluctuating fuel prices have forced carriers to operate at shrunk profit margins. Airlines charge less to be more competitive with other budget airlines and maintain the market share since the flyers are price-sensitive. Even worse, the worldwide epidemic for these two years has obviously cut the number of air travellers, suppressing the revenues and even difficult sustainment for the airways. On the other hand, the Advisory Council for Aviation Research and Innovations in Europe (ACARE) issued some strategic policies aimed at enhancing European air transport to provide safety and improve fuel efficiency and clean flight. The decrease in CO2, NOx, noise emissions should be declined by 75% per passage kilometre, 90%, 65% respectively in 2050 compared to 2000 [1]. Given that CO2 emission and energy cost are directly linked to fuel consumption, airlines must invest in technological improvements to achieve substantial block fuel burn reduction and provide benefits in both economic and ecological perspectives.

To be specific, future civil aircraft engines need to take measures to boost fuel efficiency. Innovations are evolving to large fan diameter and high bypass ratio turbofans for modern engine technologies [2]. Over the past decade, designers are focusing on improving thermal and propulsive efficiency and have been approaching technology limitations [3]. Materials, cooling technology, and component efficiency are constraining further improvement of the turbofan engine performance. However, recent advances were made to break those limitations and expand the accessible design space. Consequently, it impels exploring new engine architectures with larger fans to boost propulsive efficiency by swallowing more mass flow and reducing the specific thrust.

Although the two-spool DDTF engine could minimize the fuel burn by increasing fan diameter, the fan tip speed would be unacceptable, producing substantial noise. However, reducing fan shaft speed would trigger high stage loading and impair LPT efficiency, as they share the same spool and rotate at the same speed, concluded by Larsson [4]. This consequently motivates added stage numbers for low pressure (LP) components to sustain pressure drop. Additionally, according to Dewanji [5], decreased LP spool speed could not satisfy the torque to drive the sizeable rotating fan. Thus, the LP spool is likely to be bulkier for torque relief, creating a larger core dimension. These two

facts would cause a heavier engine and consume more fuel. Therefore, the geared turbofan (GTF), three-spool or even open rotor concepts have become more appealing.

Numerous studies have been conducted to investigate advanced propulsion systems. Sieber [6] reviewed the innovative technology development in Europe and found that compared to current turbofan engine, the GTF would effectively improve propulsive efficiency from 75% to 90%, resulting in significant specific fuel consumption (SFC) reduction. Moreover, the open rotor engine demonstrated greater potential in promoting engine performance. However, it is still under development and the mature product is far from entering into service, particularly for civil aircraft. Larsson [4] performed the mission optimization of DDTF and GTF engines. It was observed that gearbox application would reduce overall engine weight, mainly by lessening the LPT stage numbers and LP shaft weight. The GTF would improve SFC and save 2.2% and 3.0% of the fuel consumption by increasing the BPR from 12.5 to 13.5 [4]. Dewanji [5] studied several GTF cases and revealed that the GTF with high BPR was effective in engine weight and SFC reduction. Alexiou [7] presented an ultra-high bypass ratio (UHBPR) GTF engine model with variable pitch fan (VPF), which showed good potential as candidate architecture at high BPR levels. Javier [8] provided a preliminary design method for GTF and constant volume combustion (CVC) GTF, reducing block fuel by 7% and 13% respectively.

Whurr [9] investigated some other competitive and applicable engine configurations, such as three-spool turbofan and open rotor engine. The three-spool turbofan incorporates an alternative shaft to separate IPC and IPT, enabling the engine to deploy more flexible matching strategies at part-load conditions. The fan diameter could also approach the ceiling without deliberating about fan tip speed and LPT counts due to the intermediate pressure (IP) shaft introduction. This allows for promoted thrust and improved SFC for the majority of thrust coming from the bypass. The lessened LPT weight could compensate for the additional weight of the third shaft. Dik [10] optimized a three-spool turbofan engine for EIS2025, saving up to 11% noticeable fuel, although the fan diameter and engine length rise 21% and 2.2% respectively. Zhang [11] designed a very high bypass ratio three-spool turbofan, approximate 18, which could refine the SFC by 13.87% at the design point.

The open rotor engine, a propeller and core engine, is also called an unducted fan and would reach an extremely high BPR, no less than 50, which offers a marvellous propulsive efficiency. Besides, the momentum drag shows a noticeable reduction compared to conventional turbofan engine, and the associated fuel burn could achieve more than 10% saving [9]. The adoption of contra-rotating propfan provides the ability of high-efficiency sustainability at

high Mach number. Larsson [12], Salpingidou [13] and Francesco [14] discovered that the open rotor could have a dramatic SFC and block fuel reduction. Nevertheless, other challenging problems remain to tackle: installation, noise and technology readiness level (TRL). In addition, the open rotor engine is inevitably heavier due to the propellers, rear components and gearbox.

Unlike the three-spool engine and the open rotor engine, GTF engine will have a negligible impact on engine layout. The dynamic shaft characteristics would be eased compared to the three-shaft engine, and the fan would mitigate bird strike risk or erosion by contrast to propfan. A higher TRL could be achieved shortly because of installing and manufacturing convenience and mature gearbox products.

Apart from the engine configuration evolution, another significant gamechanger that could be implemented for entry-into-service (EIS) by 2025 is ceramic matrix composite (CMC) with light density and withstanding high temperature. Singh [15] suggested that the uncooled CMC material could roughly allow for 1755K of the hot gas. The CMC density is just about one-third of the currently used material, nickel-based alloys, reducing up to 50% of turbine weight, concluded by Steibel [16]. In contrast, Ballal [17] demonstrated that the blade temperature for conventional, directional and single-crystal cast alloys could only reach 1223K,1273K,1323K individually. It denotes that CMC material could relieve the cooling air requirements and cut down the engine weight, thus reducing fuel usage.

Compared to the work on GTF engine performed in Reference [4][5][7][8], this study intends to distinguish the current development limitations, exploit the not-too-distant technology, and then explore the design space for GTF engine with low specific thrust in 2025. Combined with the improvements of technology and recent advances achieved in the aerodynamic design, it senses the performance boundaries and delves deeper into generating an understanding of the iterative nature of the design process, the inherent effects of the design parameters, the feasibility of the engine designed. The pursued geared ultra high bypass ratio (GUHBPR) turbofan engine was dynamically simulated to examine the engine operability. Furthermore, the aircraft level performance assessment related to the block fuel, CO2 emission and power gearbox heat load was carried out. The payload-range diagram and fuel cost have been evaluated to further exploit the annual revenue that the GUHBPR engine would bring to the airlines.

II. Methodology

A. Design and Assessment of Framework

The increasingly high overall pressure ratio (OPR), combustion chamber outlet temperature (T4) and intake air mass flow provide growing thrust and decreasing specific fuel consumption (SFC). In order to approach the boundaries of engine performance, a robust cycle design process was launched to reach the temperature (T3 and T4) limitations based on technology level in 2025. The design and optimization process containing three parts is illustrated using the flowchart in Fig. 1.

The first part is a geared turbofan engine cycle design and optimization, which was carried out in Gasturb software. Gasturb is a gas turbine performance simulation code developed to perform cycle design, parametric analysis, optimization and transient performance prediction. The program is solving equations of flow continuity and work compatibility through the use of representative component characteristics. The system of non-linear equations is solved iteratively by implementing Newton-Raphson method [18]-[20].

After recognizing the aircraft requirements and technology level in 2025, some facts could be drawn: the expected net thrusts for critical points, the minimum ground clearance, component efficiency and cooling air fraction. The maximum available fan diameter could be derived from the ground clearance and wing geometrical restrictions. The cycle design evaluations included variables such as the fan diameter, OPR, BPR and T4. The fan diameter range used for the cycle design evaluations had as top boundary the maximum allowable value and then systematically reduced it 6 times, by -5cm at the time. The fan size is directly related to the engine inlet mass flow. The maximum intake mass flow capacity and PR occurs at top of climb (ToC) condition, which is the most demanding operating point for all compressors. Thus, this point was is selected as design point for the sizing of the fan as well as the compressors. All cycles were designed to meet the net thrust requirements at the 3 critical operating points, while respecting the technological constraints imposed on T3, T4 and turbine blade metal temperatures. The technology level selected for the cycle design exercise refers to EIS2025. It should be noted that the cooling air fractions are sized at takeoff conditions, since that is the most demanding condition in terms of peak core temperature. Combining all the above into the traditional turbofan multi-point cycle design workflow, for each fan diameter examined, all cycle parameters were set to satisfy requirements and constraints, while achieving the maximum cycle efficiency[21]. The above mentioned methodology was followed to deliver optimized cycle designs for both DDTF and GTF engine architectures.

The second part of the study investigates the engine performance from aircraft performance point of view. The flight mission performance assessment was carried out using the NASA FLOPS software to evaluate block fuel and NOx emissions. Developed by the NASA Langley Research Centre, FLOPS can efficiently undertake aircraft preliminary and conceptual design with various modules. The mission performance, including block fuel, NOx, and noise modules, is used to evaluate these factors for the optimized GTF engines. In this scenario, the engine performance surrogate model (the so-called engine deck) for the generated GTF engine is extracted from Gasturb.

The third part of the study focused on engine operability and transient behaviour,which was performed using Simcenter Amesim[22]. A selection of libraries is available for transient output simulation on gas turbines, fuel systems and electric aircraft. It is also possible to easily use predefined sections such as the flight mission envelope, compressors, turbines, combustors and nozzles. The transient model is established by defining and connecting all the components in an effort to resemble the real life scenario. This study aimed to identify and quantify critical factors influencing compressor working lines response and assess surge and stability margins. Furthermore, the heat load released from the power gearbox (PGB) was assessed at different flight segments.

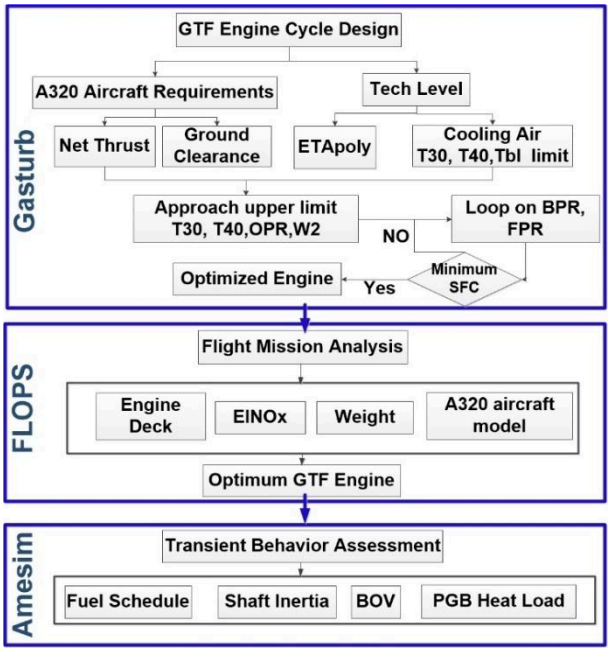

Fig. 1 GTF engine design and optimization process.

The specific case study involves a 150-seat aircraft and a typical mission profile of 2600 nm. The reference engine used is the two-spool DDTF engine, CFM56-5B-type, powering the A320-type aircraft. In this scenario, it is assumed that both the CFM56B reference engine and the newly designed engines are powering the same aircraft. To

be specific, the net thrust and flight conditions at all 3 points and flight range are identical for the two engines. The flight conditions and desired net thrusts for the 3 critical points are specified in Table 1.

Table 1 A320-type aircraft net thrust requirements[23]

Items	CR	ToC	TO
Altitude (ft)	35000	35000	0
Ma	0.78	0.78	0
ΔT_{ISA} (K)	0	10	0
Net thrust (kN)	21.2	25.3	120

B. Design Boundaries

The technology level at 2025 has set restrictions on the variables. It is assumed that the ground clearance could reach 0.5m with technology development. Thus, the fan diameter would peak at 1.9m [24], as listed in Table 2. T4 reveals the highest temperature in the gas turbine system and significantly impacts the thrust and blade life cycle. Kyprianidis [25] proposed that T4 is predicted to increase 10 K per year. It is presumed to be 1950K in 2025 by applying CMC blade and effective cooling methods. Considering the reliability of HPC last stage blade, T3 is assumed to be restricted to 950K [12]. The upper bounds for T3, T4 and T41 approach their limiting values at TO. Considering the tip leakage losses, the blade span of the last stage is suggested to be greater than 10mm. Besides, stage loading, blade tip speed, AN^2 and gear ratio for LP systems should be deliberated in view of noise production, mechanical integrity and blade stress.

Table 2 Design space constraints [12][26][27][28]

Parameters	Value
Dfan max (m)	1.9
T3max (K)	950
Tbl (K)	1250
T41max (K)	1850
T4max (K)	1950
h_{HPC}, assumed (mm)	10
Utip,max (m/s)	460
ψ_{fan}	0.3~0.6
ψ_{LPT}	3
AN^2max (m^2/s^2)	13000
Gearbox efficiency	99.42%
GR	4.5

C. Design Variables

A group of GTF engines, with a fan diameter of 1.6m to 1.9m and an interval of 0.05m, would be configured according to the developed approach in Figure1. Considering the cruise segment dominates the flight range and consumes most of the energy, it is chosen to be the design point for saving fuel. The intake air mass flow W2 could be determined at the point where the maximum intake flow capacity occurs, as suggested by Walsh [29] and Saravanamuttoo[30]. ToC is the highest power setting state and was picked to size the fan. W2 at ToC is directly connected to fan diameter from Equation (1) with the recommended inlet axial Ma being 0.6, the hub/tip ratio is 0.3 [31]. The maximum swallowing mass flow capacity is estimated to be 182 kg/s with flight Mach number of 0.78. The initial ideal FPR mainly affected by Fs would be originated from Guha Equation (2) [32] where BPR is an approximate value.

$$W_2 = A_{fan} P_t \sqrt{\frac{\gamma}{RT_t}} M_a \left(1 + \frac{\gamma - 1}{2} M_a^2\right)^{-\frac{\gamma+1}{2(\gamma-1)}} \quad \textbf{(1)}$$

$$(FPR)_{op}^{\frac{\gamma-1}{\gamma}} = 1 + \frac{\gamma - 1}{2 + (\gamma - 1) M_a^2} \left[\frac{(1 + BPR)^2}{\left(BPR + \frac{1}{\eta_{KE}}\right)^2} \left(\frac{F_s}{\sqrt{\gamma RT_a}} + M_a^2\right)^2 - M_a^2\right] \quad \textbf{(2)}$$

It is critical to scale the component maps and move the design point to the peak efficiency point so that the cruise segment has the highest efficiency. The load distribution between IPC and HPC would be determined by core work split to upgrade thermal efficiency and decrease SFC. Considering the IPC surge issue, Mourouzidis [33] suggested the maximum IPC PR is no more than 0.284 times of HPC PR. OPR at cruise would be determined by reaching T3 at TO to be 950K. Similarly, T4 at CR was nominated by approaching its limit at TO.

Polytropic efficiency for EIS 2025 of each component is chosen by empirical correction method, proposed by Sebastian [34] and listed in Table3. The innovative combination of convection and film cooling could contribute to a high overall cooling effectiveness and is the currently applied cooling method. The cooling effectiveness ε F and efficiency η cool are both set as 0.7 [35]. Therefore, the cooling air fraction ϕ could be determined based on Equation (3), derived from Horlock [35]. Tg for NGV and HPT is the limit of T4 and T41. 0.08 and 0.07 were estimated to be the coolant air portion for NGV and HPT.

Table 3 Component efficiency for GTF engine [34]

Component	Recommended η_{poly}
Fan	0.956
IPC	0.923
HPC	0.930

HPT	0.901
LPT	0.924

$$\varphi = CW^{+} = 0.06428\frac{0.072\left(\frac{T_g - T_{bl}}{T_g - T_3}\right) - 0.12}{\left(\frac{T_{bl} - T_3}{T_g - T_3}\right)} \quad \textbf{(3)}$$

D. Flight Mission Assessment

Flight mission simulation ponders the performance and weight of both the aircraft and engine. Typically, a flight mission consists of five major phases: take-off, climb, cruise, descent and landing. The mission range was assumed to be 2600nm, as seen in Fig. 2. Apparently, the cruise phase dominates the whole flight mission. NASA FLOPS software, developed by the NASA Langley Research Centre, is employed to conduct flight mission analysis. It can efficiently undertake aircraft preliminary and conceptual design with various modules.

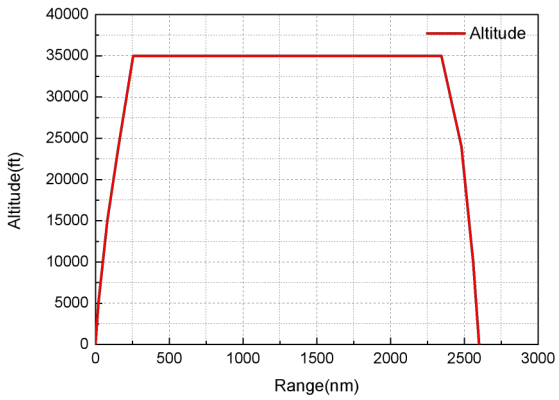

Fig. 2 Simplified flight envelop for Airbus A320

The mission outcome, including block fuel, NOx emissions, and noise modules, is used to evaluate the optimized GTF engines. NOx is estimated by the NASA P3T3 method, as shown in Equation (4) [36].

$$EINO_x = 33.2\times\left(\frac{P_3}{432.7}\right)^{0.4}\times EXP\left(\frac{T_3 - 459.67 - 1027.6}{349.9} + \frac{6.29 - 6.3}{53.2}\right) \quad \textbf{(4)}$$

A brief weight breakdown for A320 aircraft is shown in Table 4.

Table 4 Aircraft weight breakdown [37]

Parameters	Weight (kg)
Aircraft Structure	20071
Basic MEW	35774
Basic OEW	40793
MRW	73675
MTOW	73607

III. Results and Analysis

E. GTF Engine Cycle Design Results

Seven GTF cases with regard to the fan diameter were optimized according to the proposed design process. The related results for critical parameters and engine performance are shown in Fig. 3 and Fig. 4.

Figure3 shows an overall trend of the Fs, BPR, FPR and T4 for the investigated cases. The specific thrust varies from 167.6 to 119.6 N/(kg/s) for the increased intake mass flow when fan diameter grows from 1.6m to 1.9m, as shown in Figure3. It has been proved that the Fs is the decisive factor that influences the engine parameters choices [32]. The graph shows that there has been a slight fall in the FPRop while a steep rise in BPR and T4, when the Fs falls. The achievable BPR reaches the peak of 13.15 with the corresponding T4 of 1687K since the T4 has to rise to compensate for the declined core thrust. However, the higher BPR and corresponding T4 generate an apparent demand in cooling air to protect the turbine blade from failure and extend the engine life. Nevertheless, increasing the cooling fractions would eventually offset the benefits of utilizing high BPR and T4. As mentioned above, the turbine cooling air is designed to satisfy the most demanding operation which appears at the takeoff segment. Finally, the FPR design value that provides the optimum SFC and Fs would decrease as the fan diameter increases.

It should be noted that there would be obvious changes in the fan characteristic map, resulting from the fan diameter variation. For the larger fan diameter case, the FPR becomes lower while the peak efficiency area and the surge line moves downwards. Meanwhile, the corrected mass flow would be increased due to the enlarged intake mass flow. However, longer fan blades might pose aerodynamic instability problems. A wide-chord fan blade would be preferred to avoid the possible flutter issue.

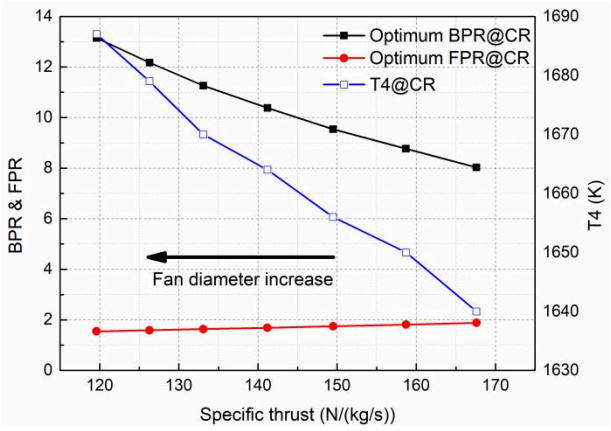

Fig. 3 FPRop, BPRop and T4 for different fan diameter

The estimated thermal and propulsive efficiency are compared in Fig. 4. At between 1.6m and 1.9m fan diameter, the thermal efficiency is extremely flat, with an average value of 0.52 because T3 and T4 approach the maximum acceptable values. As the fan diameter grows from 1.6m to 1.9m, the propulsive efficiency at CR rises by 8.19%, leading to a 7.47% improvement of SFC and 28.64% decrease in specific thrust, as shown in Figure5. Apparently, propulsive efficiency variation dominates the enhancement of SFC. It seems that GTF engine with a fan diameter 1.9m is the best candidate for EIS 2025 for its lowest SFC and specific thrust.

Nevertheless, it is not reasonable to pick the ideal engine only by SFC, since the weight penalty should not be ignored, as shown in Fig. 5. Compared to the engine with fan diameter 1.6m, the engine with fan diameter 1.9m was found heavier by 12.74%. Therefore, weight penalty would be considered in the flight mission performance assessment.

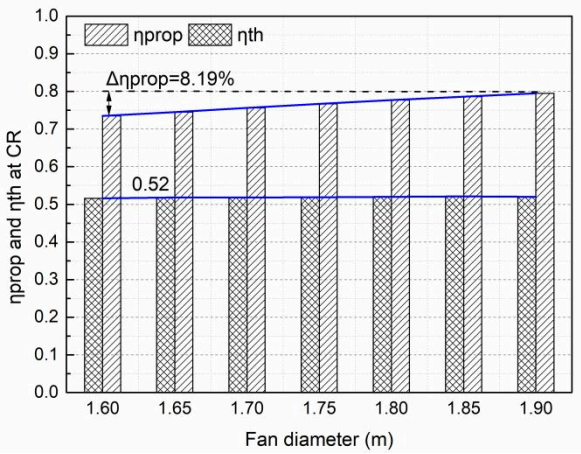

Fig. 4 Propulsive and thermal efficiency

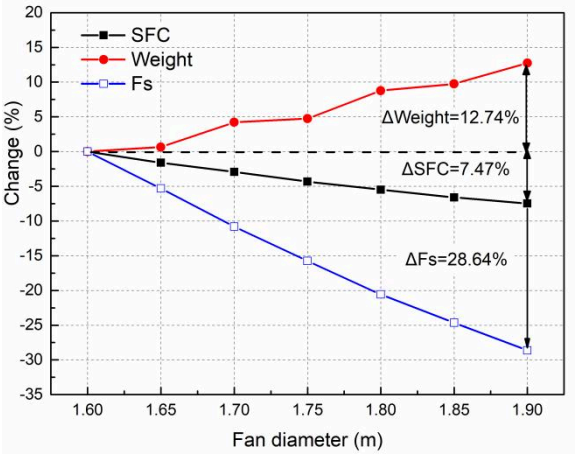

Fig. 5 Engine performance change rate

F. Flight Mission Performance

The flight mission simulation results for 2600nm are depicted in Fig. 6 to Fig. 8. An obvious observation is that enlarging fan diameter would contribute to reducing the SFC and fuel burn despite the weight offset. Another finding is that the SFC reduction rate is slightly greater than the block fuel, reaching 7.47% and 6.58% respectively due to the growing engine weight penalty, seen in Fig. 7. In terms of noise, it declines from 161.97 dB to 156.6 dB, when moving from 1.6m to 1.9m fan diameter, as presented in Fig. 8. The lowered fan tip speed is the main contributor to noise suppression, which will be detailed in the next sections. However, similar fan diameter increase yields an increase in NOx emissions by 5.49%, from 221.36kg to 233.52kg. In this scenario, reliefing the NOx emissions entails the introduction of low NOx emission combustor, such as the Twin annular premixing swirler (TAPS) [38].

Hence the optimum engine is bound to be with fan diameter of 1.9 m, which was nominated as the geared ultra-high bypass ratio (GUHBPR) turbofan engine.

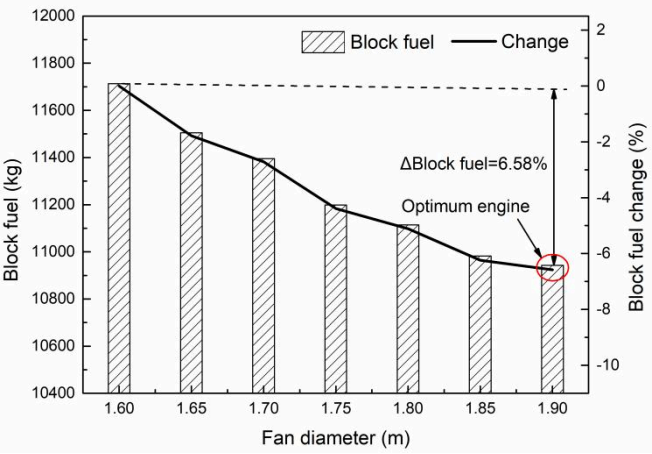

Fig. 6 Block fuel for different fan diameter

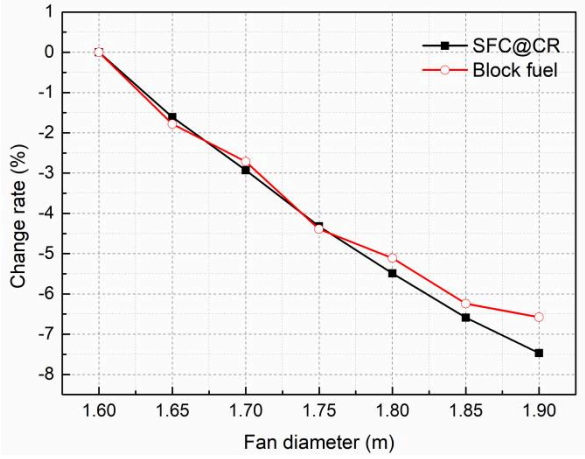

Fig. 7 SFC and block fuel change rate

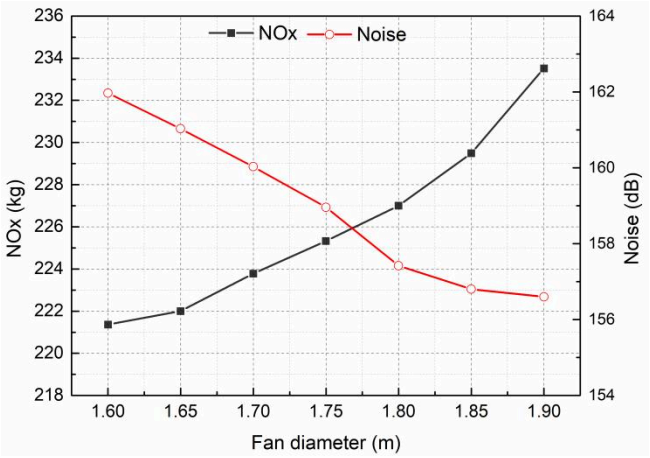

Fig. 8 Emissions for different fan diameter

G. Aircraft Level Performance Comparison with DDTF engine

The configuration comparison of the developed GUHBPR and the DDTF engine is depicted in **Fig. 9**. Apparently, the GUHBPR is shorter than the DDTF and the LPT counts are significantly reduced. In addition, the size of HPC and booster for the GUHBPR are minimized. The advantages of implementing GUHBPR are assessed relative to the DDTF engine regarding the economy and environment, to confirm whether it is consistent with the target of ACARE.

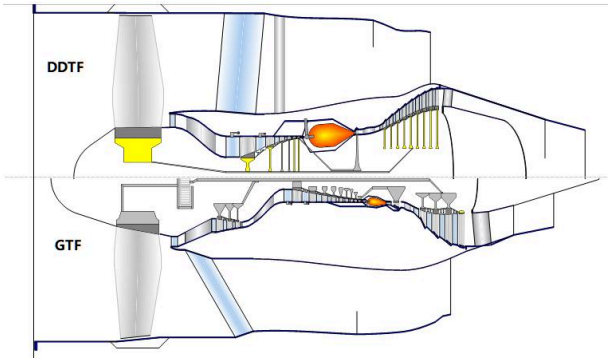

Fig. 9 GUHBPR engine and DDTF engine

1. 2600nm mission comparison

The overall block fuel for GUHBPR engine has dramatically decreased by 30.85%, as listed in Table 5. Simultaneously, the declined block fuel at cruise approaches 29.55%. It indicates that most of the saved fuel originates from the tremendous reduction in SFC at cruise and engine weight, reaching 27.85% and 26.33% respectively. The apparent engine weight reduction mainly results from the decreased LPT counts, minimized HPC and booster, Resin-matrix composites fan blade and the shortened engine length. The developed engine cycle design method has successfully approached the performance boundaries and led to tremendous improvement in SFC.

When it comes to emissions, NOx rises by 37.12% for the elevated combustor inlet pressure and temperature. The generated noise almost remains unchanged while the benefit of declining CO2 reaches up to 30.85%. Based on the same installed aircraft, the GUHBPR engine shows massive advantages and considerable potential to be employed for EIS2025.

A further analysis was performed to figure out the primary reason for the significant block fuel saving. The GUHBPR engine weight is assumed to be the same as the DDTF engine, 2355kg, block fuel would still drop by 29.77%, as shown in Table 6. It highlights the crucial role of lowering the SFC at cruise segment in enhancing the fuel economy.

Table 5 Comparison between GUHBPR and DDTF engine

Performance	DDTF	GUHBPR	$\frac{GUHBPR-DDTF}{DDTF}$ (%)
B_{fuel} (kg)	15824	10943	-30.85
B_{fuel} at CR (kg)	9614.5	13647	-29.55
SFC at CR ((g/s)/kN)	17.52	12.64	-27.85
NOx (kg)	170.3	233.52	37.12
Noise (dB)	156.14	156.6	0.29
CO_2 (kg)	49022	33901	-30.85
E_{weight} (kg)	2355	1735	26.33

Table 6 Block fuel for the same given engine weight

Item	DDTF	GUHBPR	$\frac{GUHBPR-DDTF}{DDTF}$ (%)
Range (nm)	2600	2600	0
Given E_{weight} (kg)	2355	2355	0
B_{fuel} (kg)	15824	11113.2	-29.77

2. Operating economics

For a fair comparison of the aircraft performance, the gross weight (GW), maximum fuel capacity, operating empty weight (OEW) are assumed to be the same for the DDTF engine and the GUHBPR. The payload-range diagram is illustrated in Fig. 10. The published data for A320-type aircraft is also presented as the grey dash line [23]. B is the point where gross weight (GW) and payload are simultaneously the maximum values. 1905.4nm and 2799.4nm could be achieved for DDTF and GUHBPR at point B. The GUHBPR could provide superior payload-range capacity with an extended flight range, approaching a 45% increase in range relative to the DDTF engine.

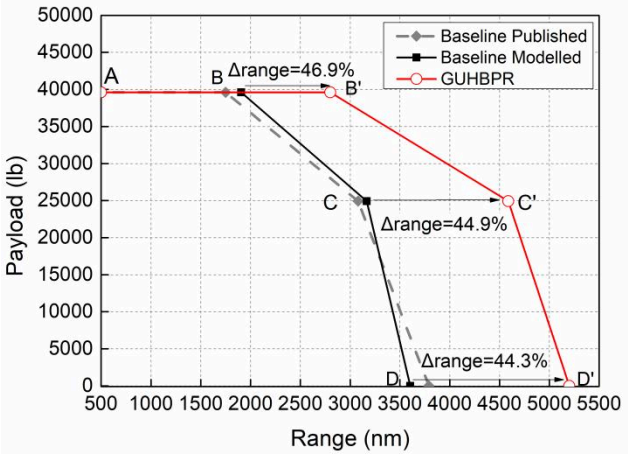

Fig. 10 Payload-range diagram

To further explore the advantages of using the GUHBPR, five specific missions, 500nm, 1000nm, 1500nm, 3000nm, 3500nm, were simulated in terms of block fuel, CO2 per passenger kilometer and annual fuel cost. According to the obtained payload-range diagram in Fig. 10, the implemented methodology for different ranges is described as follows [39]:

1) As the flight range increases from A-B or A-B', the payload is kept fixed to the maximum value and the take-off weight (TOW) is gradually rising until reaching the maximum take-off weight (MTOW).
2) Then from B-C or B'-C', the TOW is kept fixed to the maximum value whereas the payload has to decrease to offset the increase of fuel burnt.
3) Finally, from C or C' to the ferry range, the payload is further minimized all the way to zero, the fuel tanks are full capacity and the aircraft flies the loingest range it can possibly achieve.

The results of the correlational analysis for block fuel and CO2 are set out in Fig. 11 and Fig. 12. It was identified that the developed GUHBPR has significant potential for fuel economy improvements for each investigated range. The extended flight range of GUHBPR would provide a 25.14% improvement in fuel economy and CO2 per passenger kilometer for the 3500nm mission comparable to the current CFM-56 engine. This value satisfies the environmental targets in 2025 for aviation in Europe (relative to the year 2000), 25% of which is required to come from the contribution of the engine [3].

The resulted annual fuel cost saving is summarized in Fig. 13. The flight frequency is assumed to be one flight per day for each range. Meanwhile, considering the possible fuel charge fluctuation, the estimated fuel price ranges from 1 USD to 4 USD per gallon [40]. Fig. 13 is revealing an economic characteristic of the GUHBPR, in terms of annual fuel based cost savings. What stands out is that a longer flight mission would support the airlines in

achieving more profits. Furthermore, a higher fuel price would highlight the benefits of using the optimized engine. The GUHBPR was identified to be a fuel-efficient and eco-friendly engine for EIS2025.

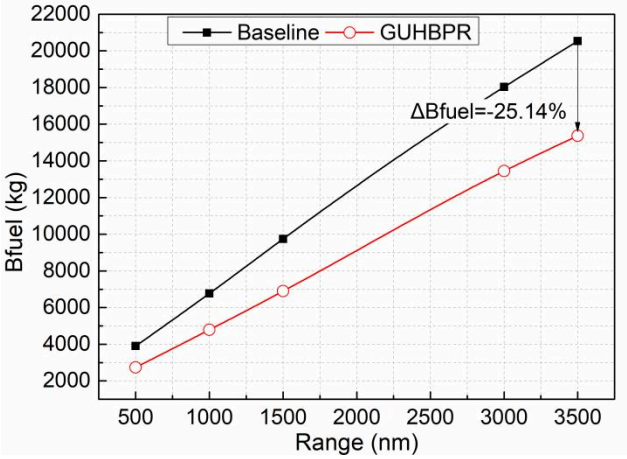

Fig. 11 Block fuel comparison for different ranges

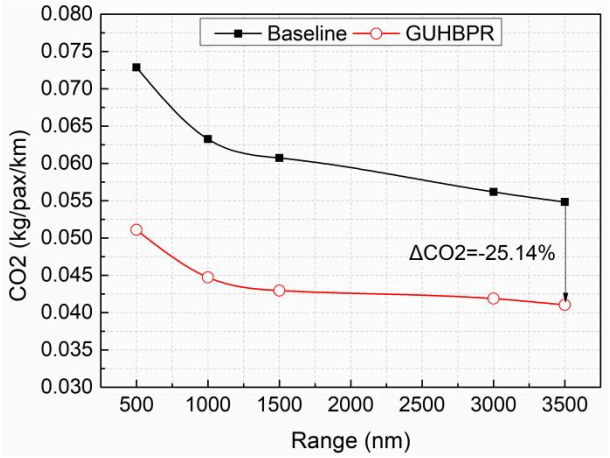

Fig. 12 CO2 emission comparison for different ranges

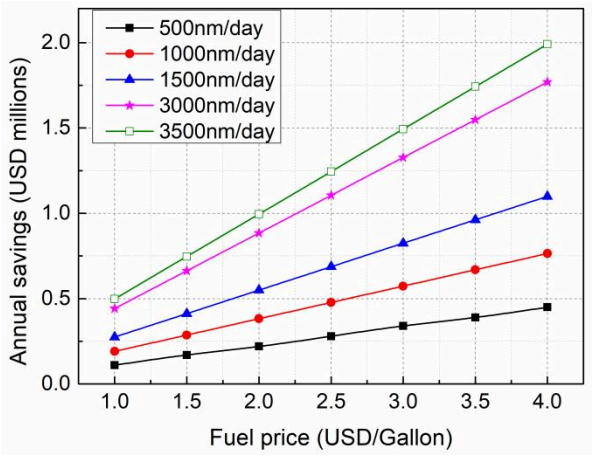

Fig. 13 GUHBPR annual savings for fuel cost

H. CMC application

In this study, CMC was introduced into HPT and LPT vanes and blades of the GUHBPR engine [41]-[43]. The application of CMC for turbine blade in the year 2025 might be a little aggressive. However, the industry, such as GE and Pratt & Whitney are eager to develop applicable CMC turbines within a short time. It might be achievable in the near future.

The density of Inconel 718 is substituted by CMC when calculating the engine weight. The same optimization process is implemented in the CMC equipped engine in seeking the maximum benefits, as shown in Table 7. Apparently, maintaining the same T4, the increase of permitted metal temperature leads to the reduction in cooling air requirement, resulting in the boost of thermal efficiency. Besides, the 17.95% enlarged BPR for the CMC engine enhances the propulsive efficiency. Therefore, there is a 3.8% betterment in SFC for the cruise condition. Combined with the 2.77% decrease in engine weight, the saved block fuel is 4.93%. Meanwhile, besides the significantly higher temperature tolerance, CMC's present lower density which obviously relieves the turbine blade stress concentration and further extend the engine life.

Table 7 Performance comparison for the GUHBPR engine with CMC and Inconel 718

Material	Inconel 718	CMC	$\frac{CMC-\text{Inconel 718}}{\text{Inconel 718}}$ (%)
D_{fan}(m)	1.9	1.9	0
BPR at CR	13.15	15.51	17.95
T4 at CR(K)	1687	1690	0.18
T4 at TO(K)	1950.0	1950.5	0.026
Tbl (K)	1250	1755	40.4
E_{weight} (kg)	1735	1687	-2.77
SFC at CR((g/s)/kN)	12.64	12.16	-3.80

Furthermore, the mission performance refinement of the GUHBPR with CMC material is shown in Fig. 14. In spite of the magnificent benefits of Inconel GUHBPR compared to the DDTF engine, the CMC enjoys a further 4.93%, 5.90%, 0.98% reduction in block fuel, NOx and noise. It turns out that CMC is a promising material that could significantly boost engine performance.

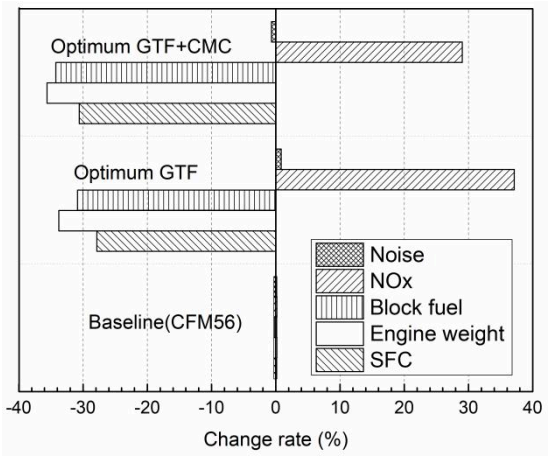

Fig. 14 Performance improvement

IV. Engine Operability Assessment

I. Feasibility Examination

A well-designed engine should not only have superb aerothermal performance but needs to operate safely throughout the flight envelope. The Fan and IPC are especially prone to surge at low corrected speed due to the large incidence angle, causing reversal flow, vibration and even flame-out [30]. In this scenario, the following interventions are tested to prevent such accidents: blow-off valve (BOV) bleed, variable inlet guide vane (VIGV), variable area nozzle (VAN). The impacts of programmed BOV bleed control, bypass VAN and 42° VIGV are presented in Fig. 15, revealing that they could effectively prevent IPC from surge.

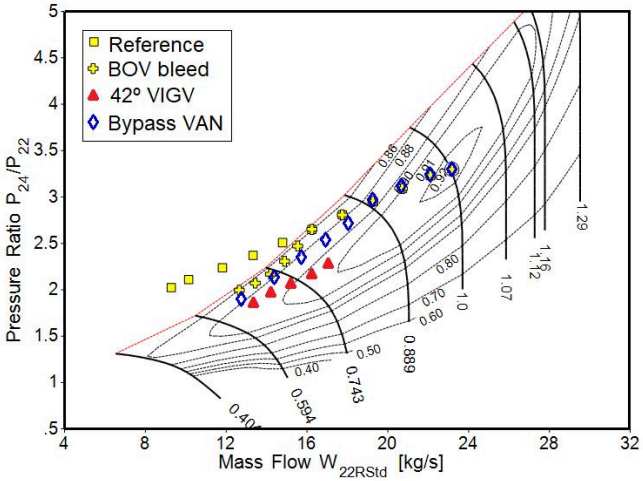

Fig. 15 BOV, bypass VAN and VIGV effects

The mutual relationship of fan tip speed, LPT AN^2 and gear ratio has constrained and determined the feasibility of LP system. Meanwhile, stage loading and HPC last stage blade height are accounted during the design. The

general trend for $U_{Fan,tip}$ showed that it decreases with fan diameter increase and in none of the designs it resulted to be greater than 460m/s.This indicates that moderate centrifugal stress and noise level are produced by all engine designs. Regarding AN^2, the primary consideration for is the LPT mechanical integrity. All engine designs resulted to be lower than the limitation of 13000 m^2/s^2, thus remained within the safety margin. Finally, the resulted gear ratio ranges from 2.5 to 2.2.

Stage loading reveals energy exchange, and a high stage loading might induce excessive turning and Mach number increase, but would be restricted by the aerodynamics of the blade. Stage loading should not be too high to induce shockwave. As fan diameter rises from 1.6m to 1.9m, fan stage loading decreases from 1.04 to 0.52. However, only the engines with DFan 1.85m and 1.9m are acceptable. The maximum LPT stage loading is 2.7 and satisfies the requirement. Finally, the HPC last stage blade height is above the lower bound, which mitigates the leakage loss and efficiency degradation.

Table 8 Feasibility examination

D_{Fan} (m)	$U_{Fan,tip}$ (m/s)	ψ_{Fan}	AN^2 (m^2/s^2)	ψ_{LPT}	GR	h_{HPC} (mm)
1.6	435	1.04	12149	2.64	2.2	12
1.65	445	0.77	12368	2.61	2.2	11
1.7	433	0.73	12713	2.34	2.3	10
1.75	440	0.68	12065	2.55	2.3	10
1.8	397	0.69	11522	2.62	2.5	10
1.85	404	0.6	10786	2.73	2.5	12
1.9	410	0.52	10623	2.70	2.5	10

J. Transient Behaviour Examination

In order to examine the transient behaviour of the GUHBPR engine, this paper established several cases regarding the impacts of fuel schedule, fan shaft inertia, BOV profile. Besides, the heat load of the power gearbox was assessed at the critical flight segments to study the effects of the power losses on the engine performance and cooling system.

1. Fuel Schedule

Three cases with the fuel duration of 4s, 6s and 8s for acceleration and deceleration were established, as shown in Fig. 16. The fuel schedules are also presented in Fig. 16. The fuel flow is 0.4kg/s and 0.82kg/s in idle and take-off mode, depending on the cycle design. The effects of fuel schedule on IPC operating lines are illustrated in Fig. 17. During the acceleration, the IPC operating line moves below the steady-state (SS) point while the deceleration manoeuvre would boost the IPC pressure to pump more air to the rear component. To be specific, at the first few

instants of the acceleration, the air mass flow instantly increases. Because the HPC inertia is small, the engine begins to swallow more air. While the IP speed remains constant due to the shaft delay, the initial excursion of IPC is towards the point below the SS line. Then IPC shaft begins to speed up, and the operating line parallels the SS line and proceeds to the ultimate required speed. When performing deceleration, the original air mass flow is relatively high and could not decline immediately. IPC PR has to slightly rise to pump the intake air mass flow to the rear components. Thus, the IPC trajectory for the first instant is above the SS line. When a quick deceleration functions, the shaft delay is more prominent. The operating line proceeds much closer to the surge line, so the IPC pressure ratio would be high enough to impel the airflow that has been swallowed in the engine.

Furthermore, a slam fuel reduction would push the working line closer to the surge line due to the delayed shaft response. The minimum surge margin for the 4s case is about 15.3%, which is still within the range of 15%~20% [29]. However, the fuel profile needs to be deliberately scheduled to avoid the IPC instability.

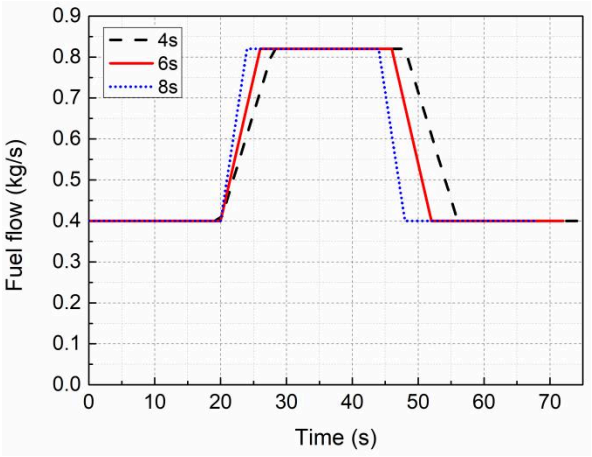

Fig. 16 Fuel schedule for the established cases

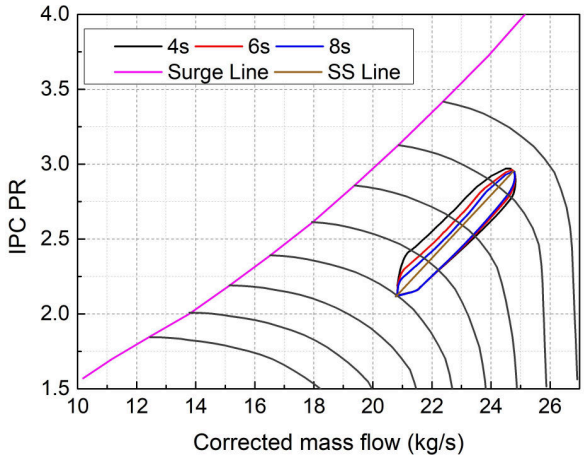

Fig. 17 IPC operating line comparison

2. Fan shaft inertia

Fan shaft inertia ranks the top of the three shafts and generates the most severe delay, which is caused by the large fan rotating mass and added gearbox. Three cases by multiplying Fan shaft inertia with 1, 1.5 and 2 were investigated to identify the variation of the engine performance. A larger Fan shaft inertia would significantly delay the IPC and the net thrust response, as depicted in Fig. 18 and Fig. 19. Meanwhile, a surge margin of 14.1% for the IFan X2 case could be observed while the IFan X1 case satisfies the requirement, indicating that the fan shaft inertia is profound in engine transient operability.

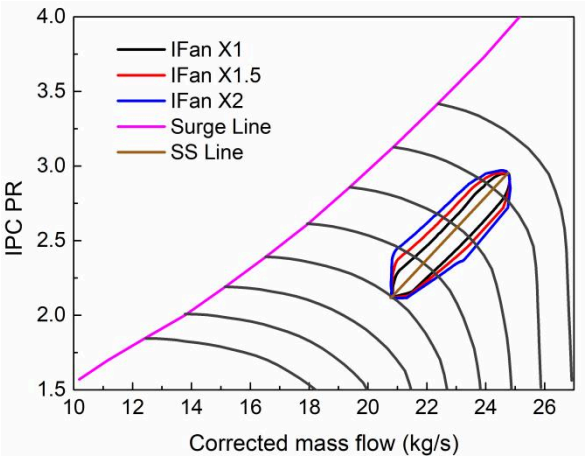

Fig. 18 IPC operating line comparison

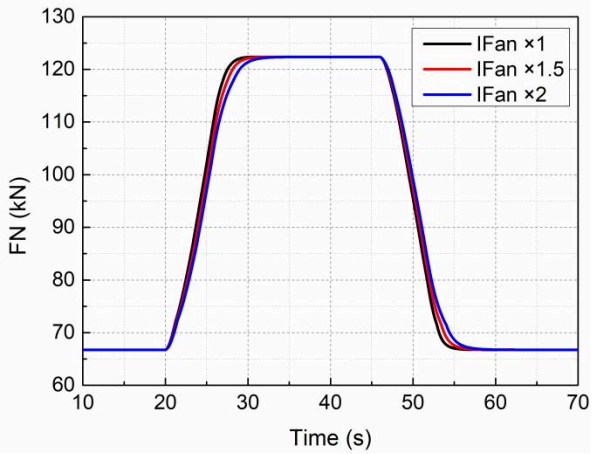

Fig. 19 Net thrust comparison

3. BOV Schedule

To obtain the BOV influences, the blow-off air fraction was reduced by 10% and 30% based on the reference BOV profile, as shown in Fig. 20. The engine behaves normally for the reference case and the lowest surge margin is about 19%. However, when the blow-off air fraction dropped by 30%, the running line obviously shifts to the

surge line and the resulted surge margin declines to 14.7%, as shown in Fig. 21. Therefore, it is of significant importance to maintain a certain level of blow-off air, especially at the low corrected speed.

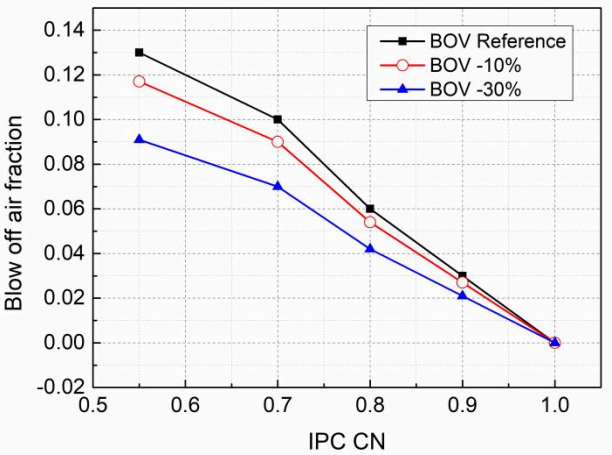

Fig. 20 BOV schedule

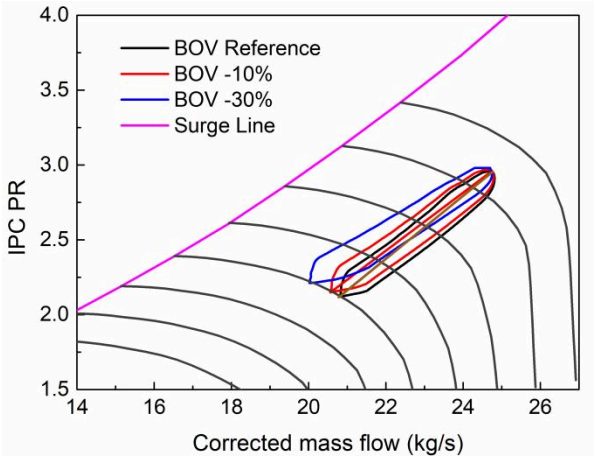

Fig. 21 IPC operating line comparison

4. Heat Load Estimation

PGB functions as the transmitter to transfer the IP shaft power to Fan shaft power. A higher gearbox efficiency would entail less input power and produce lower heat rejection. The generated heat in the PGB during engine operation could be deemed a form of power loss. Consequently, the reduced power loss would be beneficial for decreasing fuel consumption and mitigating thermal management. The examined power losses for gearbox during the specific flight mission are demonstrated in Fig. 22. The power input at TO and climb are approximately 17MW and 15MW, while the losses take up about 1.07% and 1.12%. In terms of ToC and cruise, the losses reduce more than half of those at TO and climb. It could be concluded that the gearbox heat is important throughout the mission and may pose a critical parameter for low power rating operation and the thermal management design.

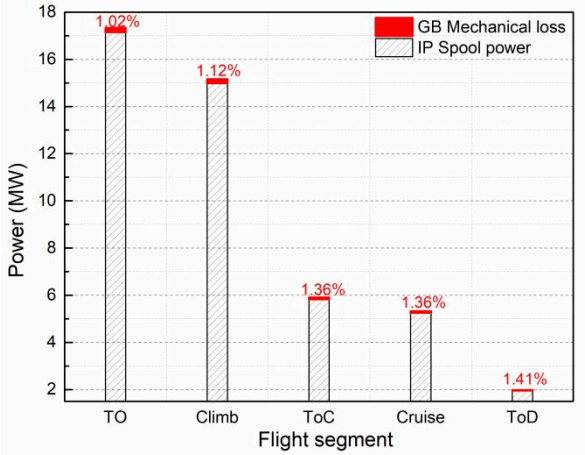

Fig. 22 PGB heat load for critical flight segments

V. Conclusion

This study launched a robust design process of a low specific thrust GTF engine to seek a fuel-efficient engine within the design limits, dedicated to achieving low operating costs and environmental impact. The methodology was introduced and consistently accomplished in three well-established tools. The findings indicate the apparent advantages of the geared turbofan over the two-spool DDTF engine. The most compelling engine layout for 150 pax A320-type aircraft was proposed for EIS 2025. The main outcome of this paper is summarized as below:

1. The proposed design optimization process provides a deeper insight into the low specific thrust engine design and proves to be a promising approach in obtaining the optimum performance. Fan diameter is the major constraint to lessen the fuel burn. The assessment of the performance boundaries demonstrated that specific thrust reductions always contribute to better engine performance consuming less fuel in a designated mission. The highest possible thermal efficiency was achieved by approaching T3 limit at TO while the propulsive efficiency was boosted by the enlarging BPR. Compared to the DDTF engine, the pursued GUHBPR engine attained a 27.85% improvement in SFC and a 30.85% reduction in block fuel and CO2 of the 2600nm mission.

2. From the perspective of financiers, the aircraft equipped GUHBPR engine covers a more extended flight range based on its payload-range capability. Further analysis from multi-range views proves that a longer flight mission would attain more cost advantages. Furthermore, a higher fuel price would highlight the benefits of using the GUHBPR engine. For 4 USD/gallon fuel charge, the annual fuel cost saving of 3500nm mission reaches 2 USD millions. A 25.14% fall in CO2 per passenger kilometer has met the environmental targets in 2025. The GUHBPR was identified to be a fuel-efficient and eco-friendly engine for EIS2025.

3. The implementation of CMC turbines offers additional benefits in minimizing engine weight, SFC and block fuel. With its lighter density, the overall GUHBPR engine weight was reduced by 2.77%. The splendid high-temperature tolerance capacity provided significant cooling air relief and 3.8% of SFC improvement. As a consequence, a 4.93% reduction in block fuel was achieved, revealing the promising prospect of deploying CMC material for civil aircraft.

4. Feasibility check of engine cycle design implied the GUHBPR engine could operate effectively with Fan tip speed, AN^2, stage loading and HPC last stage blade height within the bounds. Dynamic simulation of GUHBPR was further performed to examine the engine operability. Fan shaft inertia is the dominant factor influencing GUHBPR engine transient behaviour. However, fuel scheduling and BOV profiles should be given a moderate schedule to ensure IPC stability. Finally, the PGB heat load is also critical, especially at low power ratings and the related fuel-oil cooling system would need modification.

Acknowledgments

The authors would like to thank AECC Shenyang Engine Research Institute for the fund and Cranfield University for the support.

References

[1]. Darecki, M., Edelstenne, C., Enders, T., Fernandez, E., Hartman, P., Herteman, J.-P., Kerkloh, M., King, I., Ky, P., Mathieu, M., Orsi, G., Schotman,G., Smith, C. and Wörner, J.-D. (2011). Flightpath 2050, Flightpath 2050 Europe's Vision for Aviation, p. 28. https://doi.org/10.2777/50266.

[2]. Hughes C. (2011). The promise and challenges of Ultra High Bypass Ratio engine technology and integration, AIAA Aero Science Meeting, NASA Glenn Research Center, 2011.

[3]. Realising Europe's vision for aviation, Strategic Research & Innovation Agenda (Sep 2012), ACARE, available at: http://www.acare4europe.org/sites/acare4europe.org/files/attachment/SRIA%20Volume%201.pdf, 2012.

[4]. Larsson, L., Avell, R. and Gronstedt, T. (2011). Mission Optimization of the Geared Turbofan Engine, ISABE-2011-1314, pp. 1-7.

[5]. Dewanji, D., Rao, G. A. and Van Buijtenen, J. (2009). Feasibility study of some novel concepts for high bypass ratio turbofan engines, Proceedings of the ASME Turbo Expo, 1(0), pp. 51–61. https://doi.org/10.1115/GT2009-59166.

[6]. Sieber, J. (2015). European Technology Programs for Eco-Efficient Ducted Turbofans, ISABE, (20029). https://doi.org/10.1145/3132847.3132886.

[7]. Alexios A., Nikolaos A. Roumeliotis I., etc. (2017). Performance modelling of an ultra-high bypass ratio geared turbofan. ISABE-2017-22512, pp. 1-12.

[8]. Javier Oliva V. (2011). Computer modelling of aircraft performance for trajectory and mission optimization for civil aviation, MSc Thesis, Cranfield University, 2011.

[9]. Whurr, J. (2013). Future Civil Aeroengine Architectures & Technologies (presentation), 10th European Turbomachinery Conference, Lappeenranta, Finland, April 2013.

[10]. Dik, A., Bitén, N., Zaccaria, V., Aslanidou, I. and Kyprianidis, K. G. (2017). Conceptual Design of a 3-Shaft Turbofan Engine with Reduced Fuel Consumption for 2025, Energy Procedia. Elsevier B.V., 142, pp. 1728–1735. https://doi.org/10.1016/j.egypro.2017.12.556.

[11]. Zhang F. (2019). Conceptual design of a three-shaft high bypass turbofan engine for entry-into-service 2025. MSc Thesis, Cranfield University. 2019.

[12]. Larsson, L., Larsson, T, L., Grönstedt, T. and Kyprianidis, K. G. (2011). Conceptual design and mission analysis for a geared turbofan and an open rotor configuration. Proceedings of the ASME Turbo Expo, 1, pp. 359–370. https://doi.org/10.1115/GT2011- 46451

[13]. Salpingidou, C., Misirlis, D., Vlahostergios, Z., etc. (2018). Conceptual design study of a geared turbofan and an open rotor engine with intercooled recuperated core. J Aerospace Engineering 2018, Vol. 232(14) 2713–2720. https://doi:10.1177/0954410018770883.

[14]. Francesco S. M, Joshua S, Florian J., etc. (2019). Modelling geared turbofan and open rotor engine performance for year-2050 long-range and short-range aircraft. Journal of Engineering for Gas Turbines and Power, Paper GTP-1447, https://doi.org/10.1115/1.4045077.

[15]. Singh G., Gonczy S., Deck C., et al. (2018). Interlaboratory round robin study on axial tensile properties of SiC-SiC CMC tubular test specimens. International Journal of Applied Ceramic Technology, 2018, https://doi.org/10.1111/ijac.13010.

[16]. Steibel J. (2019). Ceramic matrix composites taking flight at GE aviation. American Ceramic Society Bulletin, Vol 98, No.3, 2019.

[17]. Ballal, D. R., Zelina, J. (2004). Progress in Aeroengine Technology (1939–2003), Journal of Aircraft, Vol.41, No.1, January-February 2004, doi:10.2514/1.562.

[18]. Gasturb. Gasturb 13.0 User Manual, 2020.

[19]. [24]Kurzke J. (2009). Fundamental differences between conventional and geared turbofans. Proceedings of ASME Turbo Expo 2009, vol. GT2009-59745, Orlando, Florida, USA, 2009.

[20]. [61]Kurzke J., Halliwell I. (2018). Reynolds Number Corrections, Propulsion and Power. Springer, Cham, 2018. https://doi.org/10.1007/978-3-319-75979-1_17.

[21]. Mourouzidis C. (2016). Cycle optimsation & preliminary design of very low specific thrust turbofan engines. Cranfield University, PhD Thesis.

[22]. Siemens, Simcenter Amesim User Manual, 2020.

[23]. Roux E. (2007). Turbofan and turbojet engines database handbook. GE-1019.004, 2007.

[24]. Aircraft characteristic airport and maintenance planning, available at: https://www.as.arizona.edu/~gschneid/ECLIPSE_WEB/TSE2015/A320_DOCUMENTS/Airbus-AC-A320-Jun2012.pdf.

[25]. Kyprianidis G. K. (2011). Future Aero Engine Designs: An Evolving Vision, Advances in Gas Turbine Technology, Dr. Ernesto Benini (Ed.), ISBN: 978-953-307-611-9, InTech, Available at: http://www.intechopen.com/books/advances-in-gas-turbine-technology/future-aero-engine-designs-anevolving-vision.

[26]. Jackson A J B. (2009). Optimisation of aero and industrial gas turbine design for the environment, PhD Thesis, Cranfield University, 2009.

[27]. Bijewitz, J., Seitz, A. and Hornung, M. (2014). Architectural Comparison of Advanced ULTRA high Bypass Ratio Turbofans for Medium to Long Range Application, DLR 340105.

[28]. Miguel Angel V.A. (2015). Preliminary design and optimisation of a power gearbox for the ULTRAFANTM geared engine. MSc Thesis. Cranfield University, 2015.

[29]. Walsh, P. P. and Fletcher, P. (2004). Gas Turbine Performance, 2nd edition, Blackwell Science Ltd, Great Britain, 2004.

[30]. Saravanamuttoo H.I.H., Rogers G.F.C., Cohen H., et al. (2017). Gas turbine theory, Seventh edition. Pearson Education Limited, Great Britain, 2017.

[31]. Moreau A., Guerin S. (2016). The Impact of Low-Speed Fan Design on Noise: An Exploratory Study. Journal of Turbomachinery. Volume 138, Issue 8, 2016. https://doi.org/10.1115/1.4032678.

[32]. Guha A. (2001). Optimisation of aero gas turbine engines. The Aeronautical Journal, 109(1049), pp.345-358. https://doi.org/10.1017/S0001924000012264.

[33]. Mourouzidis C. (2016). Cycle optimization & preliminary design of very low specific thrust turbofan engines. PhD thesis, Cranfield University, 2016.

[34]. Sebastian S, Kyprianidis G. K., Tomas G. (2015). Consistent conceptual design and performance modelling of aero engines. Proceedings of ASME Turbo Expo 2015: Turbine Technical Conference and Exposition, June 15 - 19, 2015, Montréal, Canada, GT2015-43331, pp.1-10. https://doi.org/10.1115/GT2015-43331.

[35]. Horlock J.H. (2003). Advanced gas turbine cycles. Elsevier Science Ltd, Great Britain, 2003.

[36]. Daggett, D. L. (2004). Water misting and injection of commercial aircraft engines to reduce airport NOx, NASA/CR-2004-212957, C&EA–BQ130–Y04–002, 2004.

[37]. Johannes V H. (2010). Design study of short-and medium range airliners with propfan engines, MSc thesis, Cranfield University, 2010.

[38]. Dhanuka, S.K., Temme, J.E., Driscoll, J.F., and Mongia, H. (2009). Vortex shedding and mixing layer effects on periodic flashback in a lean premixed pre vaporized gas turbine combustor, Proceedings of the Combustion Institute, 32(2):2901–2908, 2009.

[39]. Ackert S. (2013). Aircraft payload-range analysis for financiers. Technical report Aircraft Monitor.

[40]. Hensey R, Magdalina A. (2018). A320 NEO vs. CEO comparison study. FPG Amentum report.

[41]. Bakir, A S. Review on gas turbine hot section materials and technology developments. AIAA paper.

[42]. Zhu D M, Robinson C. Advanced thermal barrier and environmental barrier coating development at NASA GRC. NASA-20170005680.

[43]. Chen M W, Qiu H P, Xie W J, et al. Research Progress of Continuous FiberReinforced Ceramic Matrix Composite in HotSection Components of Aero engine. IOP Conf. Ser.: Mater. SCi. Eng. 678012043.

Assessment of performance boundaries and operability of low specific thrust GUHBPR engines for EIS2025

Mo, Da

2022-04-25

Mo D, Roumeliotis I, Mourouzidis C, et al., (2022) Assessment of performance boundaries and operability of low specific thrust GUHBPR engines for EIS2025. Journal of Engineering for Gas Turbines and Power, Volume 144, Issue 7, July 2022, Paper number GTP-21-1595
https://doi.org/10.1115/1.4054405